Naval Research Laboratory
Washington, DC 20375-5320

NRL/5610/MR—2022/3

Robust Wavefront Sensing: Experimental Demonstration of Intensity and Slopes Neural Network (ISNet)

Harshil Dave

Optical Physics Branch
Optical Sciences Division

December 22, 2022

REPORT DOCUMENTATION PAGE

Form Approved
OMB No. 0704-0188

1. REPORT DATE *(DD-MM-YYYY)*
22-12-2022

2. REPORT TYPE
NRL Memorandum Report

3. DATES COVERED *(From - To)*

4. TITLE AND SUBTITLE

Robust Wavefront Sensing: Experimental Demonstration of Intensity and Slopes Neural Network (ISNet)

5a. CONTRACT NUMBER

5b. GRANT NUMBER

5c. PROGRAM ELEMENT NUMBER
NISE

6. AUTHOR(S)

Harshil Dave

5d. PROJECT NUMBER

5e. TASK NUMBER

5f. WORK UNIT NUMBER
N2Z2

7. PERFORMING ORGANIZATION NAME(S) AND ADDRESS(ES)

Naval Research Laboratory
4555 Overlook Ave., S.W.
Washington, DC 20375-5320

8. PERFORMING ORGANIZATION REPORT NUMBER

NRL/5610/MR--2022/3

9. SPONSORING / MONITORING AGENCY NAME(S) AND ADDRESS(ES)

Naval Research Laboratory
4555 Overlook Ave., S.W.
Washington, DC 20375-5320

10. SPONSOR / MONITOR'S ACRONYM(S)

NRL/NISE

11. SPONSOR / MONITOR'S REPORT NUMBER(S)

12. DISTRIBUTION / AVAILABILITY STATEMENT

DISTRIBUTION STATEMENT A: Approved for public release; distribution is unlimited.

13. SUPPLEMENTARY NOTES

Karles Fellowship

14. ABSTRACT

This final report discusses experimental results of the intensity and slopes neural network (ISNet) for turbulent wavefront reconstruction using Shack-Hartmann data. The network was previously trained on simulated data, and transfer learning is applied to operate on benchtop experimental setup. Ground truth data was obtained using a deformable mirror to generate known turbulent wavefronts. After transfer learning, ISNet is tested on unknown wavefronts using a phase screen in the signal path. Results show improved wavefront reconstruction from ISNet compared to Shack-Hartmann reconstruction. A parallel digital holography wavefront sensor is also used to verify the results.

15. SUBJECT TERMS

16. SECURITY CLASSIFICATION OF:			17. LIMITATION OF ABSTRACT	18. NUMBER OF PAGES	19a. NAME OF RESPONSIBLE PERSON
a. REPORT	b. ABSTRACT	c. THIS PAGE			Harshil Dave
U	U	U	U	8	19b. TELEPHONE NUMBER *(include area code)* (609) 578-9791

Standard Form 298 (Rev. 8-98)
Prescribed by ANSI Std. Z39.18

This page intentionally left blank.

Robust Wavefront Sensing:
Experimental Demonstration of Intensity and Slopes Neural Network (ISNet)

ABSTRACT

This final report discusses experimental results of the intensity and slopes neural network (ISNet) for turbulent wavefront reconstruction using Shack-Hartmann data. The network was previously trained on simulated data, and transfer learning is applied to operate on benchtop experimental setup. Ground truth data was obtained using a deformable mirror to generate known turbulent wavefronts. After transfer learning, ISNet is tested on unknown wavefronts using a phase screen in the signal path. Results show improved wavefront reconstruction from ISNet compared to Shack-Hartmann reconstruction. A parallel digital holography wavefront sensor is also used to verify the results.

SECTION 1: INTRODUCTION

Adaptive optics relies on accurate wavefront sensing in order to correct for distortions to the light or image. Applications such as microscopy, astronomy, and free space communications use wavefront sensors to measure distortions from optics and atmospheric turbulence. The Shack-Hartmann wavefront sensor has been popularized due to its simplicity and fast operation [1]. However, the performance of Shack-Hartmann based wavefront reconstruction algorithms is limited in sensing distributed volume 'deep' turbulence due to large intensity variations, thus resulting in errors from scintillation. Additionally, deep turbulence results in multiple branch points on the wavefront [2], where intensity is zero and phase is undefined. These intensity variations limit, the limited ability of the Shack-Hartmann in reconstructing wavefront phase, thus motivating research into alternative wavefront sensing approaches such as Digital Holography, pyramid wavefront sensors, and others [1].

New wavefront sensing designs promise improved sensing in deeper turbulent scenarios, but the implementation of new hardware in existing AO systems induces additional costs and integration challenges. As an alternative, the wavefront reconstruction using existing Shack-Hartmann data can be improved by developing new algorithms with modern machine learning concepts. Shack-Hartmann data consists of an array of spots, the spotfield, captured on a focal plane array mounted behind the microlens array. A set of slopes is calculated from the displacement of the spots and traditional algorithms may use least squares fit and singular value decomposition [3,4] to reconstruct wavefront from slopes. Recently, various machine learning models have developed to improve the performance of Shack-Hartmann wavefront sensors. In particular, Paine and Fienup [5] use a convolutional neural net (CNN) to predict Zernike coefficients from point spread function (PSF) images. Alternatively, Swanson et al. [6] uses a U-net design to interpret x- and y-slopes to a 2D wavefront image. Hu et al. [7] uses raw spotfield data as inputs into the AI model, bypassing the centroiding step, to output the Zernike coefficients. In a previous NRL effort [8], we expanded upon the U-net design to include intensity information as an input, in addition to slopes, to create the Intensity and Slopes Network (ISNet). This additional information improved reconstruction results at greater levels of turbulence, which was demonstrated with simulated turbulence data.

For this work, we implement a pretrained ISNet model onto a benchtop experimental setup. The model is pretrained using simulated turbulence screens as described in [8]. The experimental setup serves to create new data to further train the ISNet model. Transfer learning is used to improve the network performance on experimental data. The experimental setup contains a deformable mirror, which is used to apply distortions to the wavefront and serves as the ground truth. The distorted light is detected by a Shack-Hartmann wavefront sensor as well as a Digital Holography sensor. The Digital Holography sensor serves as a secondary comparison for wavefront reconstruction accuracy.

This paper is outlined as follows. Section 2 discusses the experimental setup and transfer learning of the pretrained ISNet model on experimental data. Section 3 shows wavefront reconstruction results and comparison between the Shack-Hartmann, Digital Holography, and ISNet reconstruction method.

Manuscript approved November 22, 2022.

SECTION 2: TRANSFER LEARNING WITH EXPERIMENTAL DATA

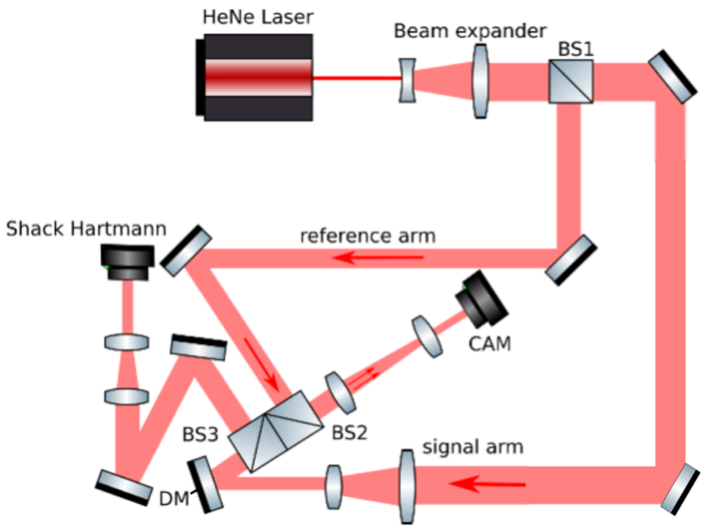

Figure 1: Experimental setup for transfer learning. A beam splitter (BS1) is used to split the signal and reference beams. The signal arm is passed to a deformable mirror (DM). BS3 is used to pick off light for the Shack-Hartmann wavefront sensor. BS2 is used to combine the reference and signal beams for the Digital Holography interference pattern, detected on the camera (CAM).

A schematic of the experimental setup is shown in Fig. 1. A 632 nm HeNe is first passed through a beam expander, then split into the reference and signal arms. The signal arm is reflected off the deformable mirror, which applies a known wavefront distortion. The reflected light is split and detected by a Shack-Hartmann wavefront sensor and also mixed with the reference arm to be detected by the Digital Holography camera. From the Shack-Hartmann sensor, the raw spotfield is recorded as well as the internally reconstructed wavefront. The raw spotfield data is used to train and validate ISNet, while the Shack-Hartmann wavefront is used as a reference for comparison. The interference fringe from the Digital Holography camera is passed through a Fourier transform based recovery algorithm to recover a direct measurement of the complex field. The Digital Holography based wavefront serves as another reference since the direct phase measurement is less prone to errors from scintillation and branch points. Calibration is performed for the deformable mirror (DM) by varying each actuator voltage, and measuring the change in phase on the Digital Holography CAM [9]. With this information, an arbitrary known phase screen can be placed on the DM.

Turbulence data is simulated by generating phase screens using Kolmogorov statistics. To simulate time-dependance in turbulence, the phase screen is generated as an infinitely long ribbon, which is pulled past the field of view, simulating a frozen flow of turbulence [10]. The set of phase screens is converted to an array of Zernike coefficients and saved in a single file. During operation, the Zernike coefficients are read and converted to actuator commands for the DM, which consists of 97 actuators. In the experimental setup, the DM displays the turbulence screen, which is detected by the wavefront sensors. Since the DM is a continuous mirror with a limited number of actuators, branch points and phase discontinuities cannot be displayed and turbulence strength is limited. While ISNet was trained to outperform the Shack-Hartmann wavefront sensor in correcting for phase discontinuities, the experimental data generated in this report serves to transfer ISNet from operating on simulated dataset to an experimental demonstration.

Since the inputs and outputs from the simulated training data set and the experimental training data set vary, some adjustments need to be made for compatibility. First, the ISNet input array size was based on a 16x16 lenslet array for the Shack-Hartmann. In experiment, we used a 29x29 lenslet array. Rather than adding a new neural net layer to ISNet to adjust for the size difference, we can take advantage of the convolutional neural net property, where the number of weights remains the same as long as the input array size is a factor of the original size. Therefore, by upscaling the experimental dataset to 32x32, we can use ISNet without modifications. Then, we perform normalization to the experimental and simulated data set, by dividing the intensity and slopes array by the standard deviation of the slopes [8]. Next, we perform registration of the truth wavefront on the DM to the Shack-Hartmann wavefront using the Pystackreg python library. The first 15 Zernike modes are used to generate the translation and scaled rotation matrices for registration.

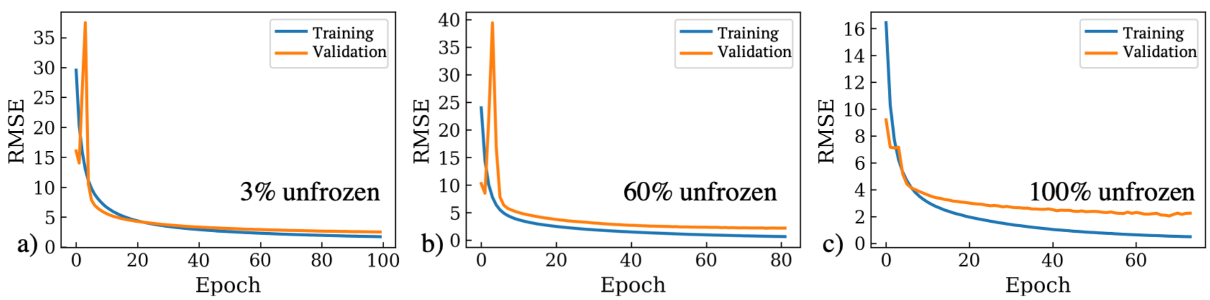

Figure 2: RMSE vs Epoch for training and validation data sets for a) 3% b) 60%, and c) 100% unfrozen layers.

To aid ISNet operation on experimental data, we employ a machine learning concept of transfer learning. We employ transfer learning by using previously trained weights from simulated data with the new experimental data. To avoid losing previously trained information, we start by freezing the weights in the neural network, and unfreezing only the top and bottom layers for learning. The learning rate, which determines the step size of the ML optimization algorithm, is also kept low (3e-5) to avoid large changes to the pre-trained network and overshooting the error minimum. Figure 2 shows the root mean square error (RMSE) versus epochs (optimization iterations) at various amounts of frozen layers. We see that unfreezing all of the layers leads to the least RMSE. In many instances, the error became worse for the first 5 epochs before improving, which is seen as the large spike in Figs. 2a and 2b. Figure 2c also shows that training error is much lower than validation error, indicating the network is overfitting, and thus ‘memorizing’ the training data. As Fig. 2 shows, it is easier to over train the neural network when all of the layers are unlocked. To avoid this, Early Stopping is used to stop training when error is no longer improving. As a result of this hyperparameter tuning, the final network is trained by unfreezing all layers and trained until Early Stopping is triggered at 70 epochs.

SECTION 3: WAVEFRONT RECONSTRUCTION RESULTS

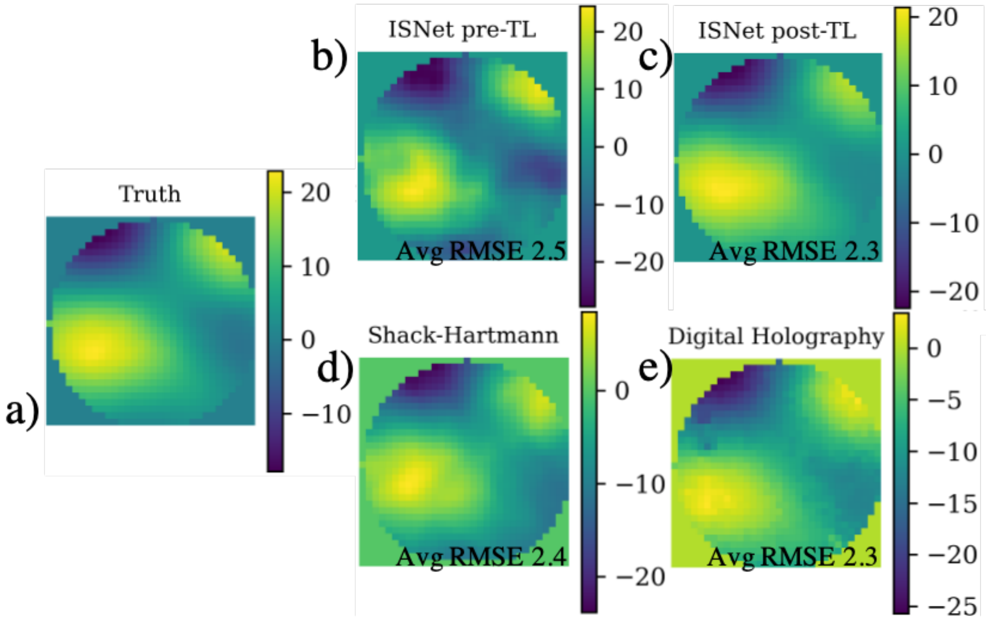

Figure 3: Comparison of reconstructed wavefronts from b) ISNet pre-transfer learning (TL), c) post-transfer learning, d) Shack-Hartmann, and e) Digital Holography, compared to a) Truth.

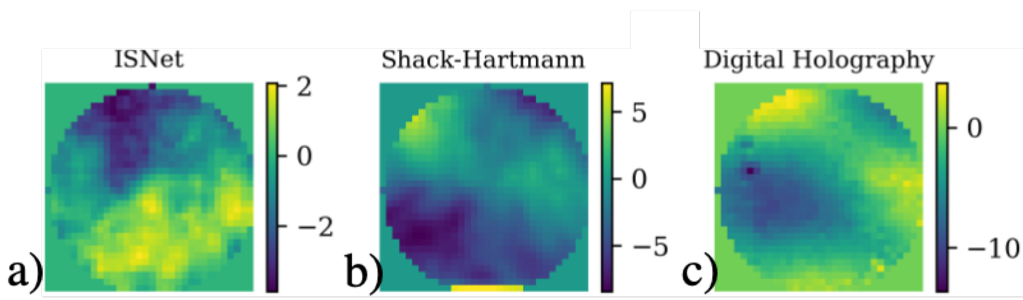

Figure 4: Difference between Truth wavefront and a) ISNet post-TL, b) Shack-Hartmann, and c) Digital Holography wavefronts.

Figure 3 shows the comparison of reconstructed wavefronts for a single realization between the Shack-Hartmann, Digital Holography, ISNet before transfer learning, and ISNet after transfer learning. The average RMSE for each measurement type over 1000 samples is calculated and displayed on the plot. Figure 4 shows the difference between the wavefront reconstruction methods and truth. Note that mean phase is subtracted when calculating the difference and RMSE. Results show that after transfer learning, ISNet is capable of enhancing the Shack-Hartmann performance, close to that of a Digital Holography wavefront sensor. Additionally, since training data includes any minor aberrations and phase shifts from relay lenses in the optical setup, ISNet error has less bias as compared to the Shack-Hartmann and Digital Holography in Fig 4. However, additional data at higher turbulence levels needs to be collected to train ISNet and quantify the merits of transfer learning.

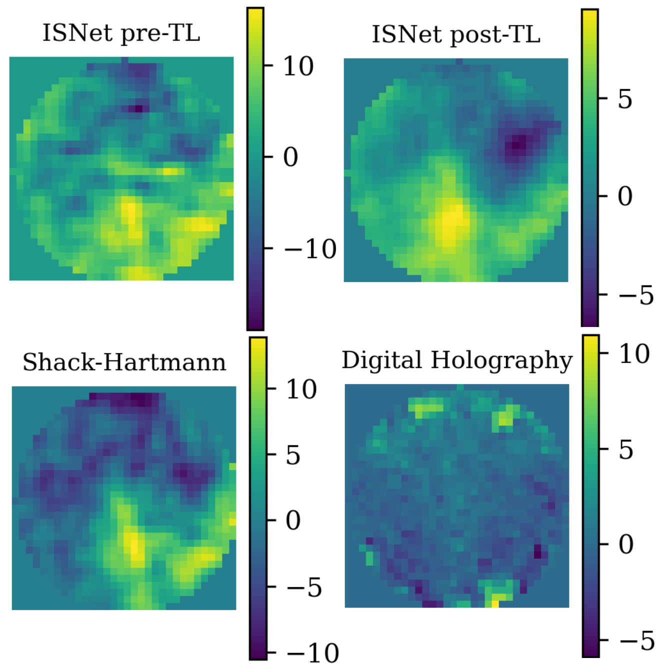

Figure 5: Comparison of reconstructed wavefronts from ISNet pre-TL, post-TL, Shack-Hartmann, and Digital Holography. Digital Holography reconstruction is not accurate due to low resolution of interference fringes. The Shack-Hartmann wavefront serves as a reference in this case.

The new model is also used to reconstruct a wavefront passed through a physical phase screen. A Lexitech phase screen with Fried parameter $r0 = 4.1$ mm is inserted in the signal path while the DM is kept flat. The $D/r0$ value of this setup is 3.2, with aperture diameter $D = 13$ mm. A greater $D/r0$ ratio would indicate a more a greater degree of turbulence. Data from the Shack-Hartmann and Digital Holography wavefront sensors is collected and compared in Fig. 6. Here, we qualitatively see that ISNet performance on experimental data is improved after transfer learning, even though it was training on limited synthetic data using a DM. Unfortunately, the Digital Holography wavefront sensor failed to capture the details of this turbulence screen, since the resolution used to capture this interference pattern was too low.

CONCLUSION

In conclusion, a machine learning model, ISNet, is demonstrated experimentally using Shack-Hartmann data. ISNet is originally trained using simulated data and transfer learning is used to optimize for experimental results. Although simulated data does not capture all real-world parameters, ISNet was trained largely using simulated data, then transferred to a real-world setup using a smaller experimental data set. The resulting performance can exceed traditional Shack-Hartmann and match digital holography reconstruction, which is demonstrated using weak turbulence levels imprinted on the deformable mirror. ISNet was also used to reconstruct an unknown turbulence screen using an experimental phase screen. For further research on ISNet performance, greater levels of turbulence should be generated in lab by using multiple phase screens and greater propagation distance.

REFERENCES

1. R. K. Tyson and B. W. Frazier, *Field Guide to Adaptive Optics* (SPIE, 2004), Vol. FG03.
2. D. L. Fried, "Branch point problem in adaptive optics," JOSA A **15**, 2759–2768 (1998).

3. W. H. Southwell, "Wave-front estimation from wave-front slope measurements," JOSA **70**, 998–1006 (1980).
4. D. L. Fried, "Least-square fitting a wave-front distortion estimate to an array of phase-difference measurements," JOSA **67**, 370–375 (1977).
5. S. W. Paine and J. R. Fienup, "Machine learning for improved image-based wavefront sensing," Opt. Lett. **43**, 1235–1238 (2018).
6. R. Swanson, M. Lamb, C. Correia, S. Sivanandam, and K. Kutulakos, "Wavefront reconstruction and prediction with convolutional neural networks," in *Adaptive Optics Systems VI* (SPIE, 2018), p. 52.
7. L. Hu, L. Hu, S. Hu, W. Gong, W. Gong, K. Si, K. Si, and K. Si, "Deep learning assisted Shack–Hartmann wavefront sensor for direct wavefront detection," Opt. Lett. **45**, 3741–3744 (2020).
8. T. B. DuBose, D. F. Gardner, and A. T. Watnik, "Intensity-enhanced deep network wavefront reconstruction in Shack–Hartmann sensors," Opt. Lett. **45**, 1699 (2020).
9. K. M. Hampson and M. J. Booth, "Calibration and closed-loop control of deformable mirrors using direct sensing," (2020).
10. D. L. Fried and T. Clark, "Extruding Kolmogorov-type phase screen ribbons," JOSA A **25**, 463–468 (2008).